

# Transition form factors and light cone distribution amplitudes of pseudoscalar mesons in the chiral quark model

A. E. Dorokhov, M.K. Volkov, V.L. Yudichev

*Joint Institute for Nuclear Research, Dubna, Russia*

**Abstract**— It is shown that a chiral quark model of the Nambu–Jona-Lasinio type can be used to describe "soft"-momenta parts of the amplitudes with large momentum transfer. As a sample, the processes  $\gamma^* \rightarrow \gamma(\pi, \eta, \eta')$  where one of the photons,  $\gamma^*$ , has large space-like virtuality is investigated. The  $\gamma^* \rightarrow \gamma(\pi, \eta, \eta')$  transition form factors are calculated for a wide region of transferred momenta. The results are consistent with the calculations performed in the instanton-induced chiral quark model and agree with experimental data. The distribution amplitudes of pseudoscalar mesons are derived.

## 1. INTRODUCTION

Effective chiral quark models (ECQM) are very useful tools for the investigation of the nonperturbative sector of QCD. Of particular interest are the Nambu–Jona-Lasinio (NJL) model and its extensions [1, 2, 3, 4, 5], where the low-energy theorems are fulfilled, and the mechanism of spontaneous breaking of chiral symmetry (SBCS) is realized in a simple and transparent way. The internal properties of the ground states of scalar, pseudoscalar, vector, and axial-vector mesons (such as masses, radii, polarizabilities, etc.) as well as all the main decays and other low-energy strong and electroweak interactions of mesons are satisfactorily described in NJL. Recently, a noticeable progress has been achieved also in constructing a  $U(3) \times U(3)$  NJL model for the description of first radial excitations of scalar, pseudoscalar, and vector mesons, including even the lightest scalar glueball [6, 7, 8].

As a rule, the NJL model is used in the low-energy physics, in particular, for the description of processes with a low momentum transfer ( $\leq 1$  GeV). And, in view of the above-mentioned success of the NJL model, it is quite interesting to extend the range of its application and to try, in particular, to describe some processes with a large momentum transfer. Indeed, for many of such processes, the factorization theorem [9, 10, 11] can be applied, which allows one to rewrite the amplitude of the process as a convolution of "hard" and "soft" parts. The "hard" part is described by the perturbative QCD (pQCD), whereas the "soft" part requires a nonperturbative approach. Usually, in QCD, the nonperturbative dynamics of quarks inside a meson is parameterized by distribution amplitudes (DA) [9], the exact form of which cannot be derived from pQCD. However, an approximation for DA can be obtained in the QCD sum rules approach (see e.g. [12, 13, 14]). On the other hand, one can calculate the "soft" part of the amplitude within a chiral quark model, where the dynamics of (constituent) quarks inside a meson is described by the corresponding quark-meson vertex instead of DA (however, one can restore the shape of DA on the base of quark-model calculations). The validity of this approach is investigated in the present work.

In our paper, we calculate the form factors that describe the transition processes  $\gamma^* \rightarrow P\gamma$  or  $\gamma^*\gamma \rightarrow P$ , where  $P$  is a pseudoscalar meson, for a wide range of transferred space-like momenta. Of interest is the kinematic region where one of the photons is not on mass-shell and has a large space-like virtuality. It is shown also that our results do not contradict both the experimental data and other theoretical models. As to experiment, we refer to the data on the  $\gamma^* \rightarrow \pi\gamma$ ,  $\gamma^* \rightarrow \eta\gamma$ , and  $\gamma^* \rightarrow \eta'\gamma$  transition processes reported by the CLEO collaboration [15]. For comparison with other theoretical models, we choose the results recently obtained in the framework of the instanton-induced chiral quark model (IQM) [16].

The structure of our paper is as follows. In Sect. 2, we introduce the  $\gamma^* \rightarrow P\gamma$  transition form factor. In Sect. 3, the part of the NJL Lagrangian describing the quark-meson interaction as well as the Lagrangian derived in the instanton vacuum model are introduced and the asymptotic behaviour of the  $\gamma^* \rightarrow P\gamma$  transition form factor for pseudoscalar mesons at high space-like virtuality of one the photons is investigated. In particular, the shapes of DA of  $\pi$ ,  $\eta$ , and  $\eta'$  mesons are found. In the last section, we discuss the obtained results and compare them with experimental data. There is also given an outlook of further possible applications of our approach.

## 2. THE $\gamma^* \rightarrow P\gamma$ TRANSITION FORM FACTOR

The transition process  $\gamma^*(q_1) \rightarrow P(p)\gamma^*(q_2)$ , where the final state mesons with the momentum  $p$  are, respectively,  $P = \pi^0$ ,  $\eta$ ,  $\eta'$ , and  $q_1$  and  $q_2$  are photon momenta, is described by the amplitude

$$\mathcal{T}(\gamma^*(q_1, e_1) \rightarrow P(p)\gamma^*(q_2, e_2)) = \mathcal{F}_P(q_1^2, q_2^2, p^2)\epsilon_{\mu\nu\rho\sigma}e_1^\mu e_2^\nu q_1^\rho q_2^\sigma \quad (1)$$

where  $e_i (i = 1, 2)$  are the photon polarization vectors;  $\mathcal{F}_P(q_1^2, q_2^2, p^2)$  is the transition form factor; and  $\epsilon_{\mu\nu\rho\sigma}$  is the fully anti-symmetric tensor.

Theoretically, at zero virtualities, the form factor

$$\mathcal{F}_P(0, 0, 0) = \frac{1}{4\pi^2 f_P} \quad (2)$$

is related to the axial anomaly [17, 18]. Here  $f_P$  is a pseudoscalar meson weak decay constant defined by the well known PCAC relation (for the pion,  $f_\pi = 93$  MeV). At asymptotically large photon virtualities, its behaviour is predicted by pQCD [19] and depends crucially on the internal meson dynamics parameterized by a nonperturbative DA,  $\varphi_P^A(x)$ , with  $x$  being a fraction of the meson momentum,  $p$ , carried by a quark.

Further, it is convenient to parameterize the photon virtualities as  $q_1^2 = -(1+\omega)Q^2/2$  and  $q_2^2 = -(1-\omega)Q^2/2$ , where  $Q^2$  and  $\omega$  are, respectively, the total virtuality of the photons and the asymmetry in their distribution:

$$Q^2 = -(q_1^2 + q_2^2) \geq 0, \quad \text{and} \quad \omega = (q_1^2 - q_2^2)/(q_1^2 + q_2^2), \quad |\omega| \leq 1 \quad (3)$$

Recent analysis of the experimental data on the form factors  $\mathcal{F}_P$  for small virtuality of one of the photons,  $q_2^2 \approx 0$ , with the virtuality of the other photon being scanned up to 8 GeV<sup>2</sup> for the pion, 22 GeV<sup>2</sup> for the  $\eta$ , and 30 GeV<sup>2</sup> for the  $\eta'$  mesons, respectively, has been published by the CLEO collaboration [15]. According to this analysis, the process  $\gamma^* \rightarrow P\gamma$  ( $|\omega| = 1$ ) can be fitted by a monopole form factor:

$$\begin{aligned} \mathcal{F}_P(q_1^2 = -Q^2, q_2^2 \approx 0, p^2)|_{\text{fit}} &= \frac{g_{P\gamma\gamma}}{1 + Q^2/\mu_P^2}, \\ g_{\pi\gamma\gamma} &\simeq 0.27 \text{ GeV}^{-1}, \quad g_{\eta\gamma\gamma} \simeq 0.26 \text{ GeV}^{-1}, \quad g_{\eta'\gamma\gamma} \simeq 0.34 \text{ GeV}^{-1}, \\ \mu_\pi &\simeq 0.78 \text{ GeV}, \quad \mu_\eta \simeq 0.77 \text{ GeV}, \quad \mu_{\eta'} \simeq 0.86 \text{ GeV}, \end{aligned} \quad (4)$$

where  $g_{P\gamma\gamma}$  are the two-photon meson decay constants.

In the lowest order of pQCD, the light-cone Operator Product Expansion (OPE) predicts the high  $Q^2$  behaviour of the form factor as follows [19]:

$$\mathcal{F}_P(q_1^2, q_2^2, p^2 = 0)|_{Q^2 \rightarrow \infty} = J_P(\omega) \frac{f_P}{Q^2} + O\left(\frac{\alpha_s}{\pi}\right) + O\left(\frac{1}{Q^4}\right), \quad (5)$$

with the asymptotic coefficient given by

$$J_P(\omega) = \frac{4}{3} \int_0^1 \frac{dx}{1 - \omega^2(2x-1)^2} \varphi_P^A(x), \quad (6)$$

where  $\varphi_P^A(x)$  is the leading-twist meson light-cone DA normalized by  $\int_0^1 dx \varphi_P^A(x) = 1$ .

In (6), the asymptotic coefficient is expressed in terms of DA. Alternatively, as it was mentioned in the Introduction,  $J_P(\omega)$  can be calculated directly either from the NJL model or from IQM. In Sect. 3, one will see that, in both models,  $J_P(\omega)$  can be rewritten in the form (6), and thus the shape of DA is extracted.

Since the meson DA reflects the internal nonperturbative meson dynamics, the prediction of the value of  $J_P(\omega)$  is rather a nontrivial task, and its accurate measurement would provide quite valuable information. It is important to note that, for the considered transition process, the leading asymptotic term of pQCD expansion (5) is not suppressed by the strong coupling constant  $\alpha_s$ . Hence, the pQCD prediction (5) can become reasonable at the highest of the presently accessible momenta  $Q^2 \sim 10 \text{ GeV}^2$ . At asymptotically high  $Q^2$ , the DA evolves to  $\varphi_P^{A,\text{asympt}}(x) = 6x(1-x)$  and  $J_P^{\text{asympt}}(|\omega| = 1) = 2$ . The fit of CLEO data for the pion corresponds to  $J_\pi^{\text{CLEO}}(|\omega| \approx 1) = 1.6 \pm 0.3$ , indicating that already at moderately high momenta this value is not too far from its asymptotic limit.

However, since the pQCD evolution of DA reaches the asymptotic regime very slowly, its exact form at moderately high  $Q^2$  does not coincide with  $\varphi_P^{A,\text{asympt}}(x)$ . At lower  $Q^2$ , the power corrections to the form factor become important. Thus, the study of the behaviour of the transition form factor at all experimentally accessible  $Q^2$  is the subject of nonperturbative dynamics. So, the theoretical determination of the transition form factor is still challenging, and it is desirable to perform direct calculations of  $\mathcal{F}_P(q_1^2, q_2^2, p^2)$  without *a priori* assumptions about the shape of the meson DA.

The asymptotic coefficient of the light-cone transition form factor in the symmetric kinematics,  $q_1^2 = q_2^2$ , ( $\omega = 0$ ) at high virtualities, is given by the integral defining  $f_P$ . In the other extreme limit, where one photon is real ( $|\omega| = 1$ ), the asymptotic coefficient is proportional to  $\int_0^1 \frac{dx}{x} \varphi_P^A(x)$  and thus is very sensitive to a detailed form of the DA.

In ref. [12], some progress was achieved by using a refined technique based on the OPE with nonlocal condensates [13], which is equivalent to the inclusion of the whole series of power corrections. By means of the QCD sum rules with nonlocal condensates, it was shown that this approach works in almost the whole kinematic region  $|\omega| \lesssim 1$ , and that for high values of the asymmetry parameter  $|\omega| \gtrsim 0.8$ , the pion transition form factor is very sensitive to the nonlocal structure of the QCD vacuum.

### 3. THE $\gamma^* \rightarrow P\gamma$ TRANSITION FORM FACTOR IN ECQM MODELS

#### 3.1. The NJL model Lagrangian

Let us consider the piece of the effective quark-meson Lagrangian that is necessary in our

calculations. It has the following form:

$$L = L_0 + L_{\text{int}} \quad (7)$$

$$L_0 = \bar{q}(i\not{\partial} - m)q, \quad (8)$$

$$L_{\text{int}} = L_1 + L_2 + L_3 + \delta L, \quad (9)$$

$$L_1 = \bar{q}i\gamma_5 \left( g_\pi \sum_{a=1}^3 \lambda^a \pi^a + g_{\eta_u} \lambda_u \eta_u + g_{\eta_s} \lambda_s \eta_s \right) q, \quad (10)$$

$$L_2 = \bar{q}i\not{\partial}\gamma_5 \left( f_\pi^{-1}(1 - Z_u^{-1}) \sum_{a=1}^3 \lambda^a \pi^a + f_u^{-1}(1 - Z_u^{-1}) \lambda_u \eta_u + f_s^{-1}(1 - Z_s^{-1}) \lambda_s \eta_s \right) q, \quad (11)$$

$$L_3 = \bar{q}\hat{Q}\mathcal{A}q, \quad (12)$$

where  $m$  is the diagonal  $3 \times 3$ -flavor matrix of constituent quark masses,  $m = \text{diag}(m_u, m_d, m_s)$ , (we consider the case of approximate isotopic symmetry  $m_u = m_d$ );  $\lambda_a$  are the Gell-Mann matrices,  $\lambda_u = (\sqrt{2}\lambda_0 + \lambda_8)/\sqrt{3}$ ,  $\lambda_s = (-\lambda_0 + \sqrt{2}\lambda_8)/\sqrt{3}$ ;  $q$  and  $\pi$  are, respectively, the quark and pion, and  $\eta_u$  and  $\eta_s$  are pure  $\bar{u}u$  and  $\bar{s}s$  pseudoscalar meson states.

The fields  $\eta_u$  and  $\eta_s$  in (10) and (11) are not physical, because they are subject to singlet-octet mixing. Here, it is assumed that the terms responsible for the singlet-octet mixing are accumulated in the term <sup>1)</sup>  $\delta L$  (see (9)), the account of which results in the following relation between "nonphysical"  $\eta_u, \eta_s$  and "physical"  $\eta, \eta'$  meson fields:

$$\eta_s = \eta \cos(\theta_0 - \theta) - \eta' \sin(\theta_0 - \theta), \quad (13)$$

$$\eta_u = \eta \sin(\theta_0 - \theta) + \eta' \cos(\theta_0 - \theta), \quad (14)$$

where  $\theta = -19^\circ$  is the singlet-octet mixing angle, and  $\theta_0 \approx 35.5^\circ$  is the ideal mixing angle [2, 20].

The quark-meson coupling constants (see [2]) are defined as follows:

$$g_\pi = g_u \sqrt{Z_\pi}, \quad g_{\eta_u} = g_u \sqrt{Z_{\eta_u}}, \quad g_{\eta_s} = g_s \sqrt{Z_{\eta_s}}, \quad (15)$$

where we introduced  $g_u$  and  $g_s$ :

$$g_a^{-2} = \frac{4N_c}{(2\pi)^4} \int \frac{\theta(\Lambda_{\text{NJL}}^2 - k^2)}{(k^2 + m_a^2)^2} d_e^4 k, \quad (a = u, s). \quad (16)$$

The integration is performed in the Euclidean metric. The divergence is eliminated by a simple  $O(4)$ -symmetric cut-off on the scale  $\Lambda_{\text{NJL}}$  that characterizes the domain of SBCS.

The terms with derivatives of meson fields in  $L_2$  (see (11)) appear because of  $\pi - a_1$  transitions [2], which also results in additional renormalization factors  $Z_a$  in  $g_\pi, g_{\eta_u}, g_{\eta_s}$ . Further, we assume that  $Z_a$  for different mesons are approximately equal (see (15)):

$$Z_{\eta_s} \approx Z_{\eta_u} \approx Z_\pi \equiv Z = \left( 1 - \frac{6m_u^2}{M_{a_1}^2} \right)^{-1} \approx 1.45. \quad (17)$$

---

<sup>1)</sup> The singlet-octet mixing appears once the pseudoscalar gluon anomaly is taken into account [2]. One can also obtain the mixing after introducing the 't Hooft term into the quark Lagrangian [20].

Here,  $M_{a_1} = 1.23$  GeV is the mass of the  $a_1$ -meson [21].

The term  $L_3$  in (12) describes the electromagnetic interaction of quarks. The photon fields are denoted by  $\mathcal{A}$ , and  $\hat{\mathcal{Q}}$  stands for the charge matrix:

$$\hat{\mathcal{Q}} = \frac{e}{2} \left( \lambda_3 + \frac{\lambda_8}{\sqrt{3}} \right), \quad (18)$$

where  $e$  is the elementary electric charge ( $e^2 = 4\pi\alpha$  where  $\alpha^{-1} \approx 137$ ).

The values of  $\Lambda_{\text{NJL}}$  and  $m_u$  are fixed by two equations [2, 20]: i) the Goldberger-Treiman relation  $m_u = g_\pi f_\pi$  and ii) the  $\rho$ -meson decay constant [2, 22, 23]

$$g_\rho = \sqrt{6}g_u \quad (19)$$

whose value 6.1 is well known from the experimentally observed decay  $\rho \rightarrow \pi\pi$ . Taking into account these equations and the expression for  $Z$  (see (17)), one finds the constituent  $u$ -quark mass:

$$m_u^2 = \frac{M_{a_1}^2}{12} \left( 1 - \sqrt{1 - \frac{4g_\rho^2 f_\pi^2}{M_{a_1}^2}} \right) \quad (20)$$

with the value  $m_u = 280$  MeV. Equating the left-hand side of (19) to its experimental value and using the definition of  $g_u$  (see (15)) with  $m_u = 280$  MeV, one obtains:  $\Lambda_{\text{NJL}} = 1.25$  GeV [2]. The mass of the strange quark is fixed by the kaon mass <sup>2)</sup>,  $m_s = 425$  MeV [20].

### 3.2. Meson transition $\gamma^* \rightarrow P\gamma^*$ form factor

Let us consider the  $\gamma^* \rightarrow P\gamma^*$  invariant amplitude corresponding to the triangle diagrams shown in Fig. 1:

$$\mathcal{T}(\gamma^*(q_1, e_1) \rightarrow P(p) \gamma^*(q_2, e_2)) = t_{P\gamma\gamma}(q_1, e_1; q_2, e_2) + t_{P\gamma\gamma}(q_2, e_2; q_1, e_1), \quad (21)$$

$$t_{P\gamma\gamma}(q_1, e_1; q_2, e_2) = -N_c g_P \mathcal{Q}_P \times \\ \times \int \frac{d^4k}{(2\pi)^4} \text{tr}\{i\gamma_5 S(k+p/2; m_a) \hat{e}_1 S(k - (q_1 - q_2)/2; m_a) \hat{e}_2 S(k - p/2; m_a)\} \quad (22)$$

where  $\mathcal{Q}_P$  depends on the electric charges and flavors of quarks that constitute the meson:  $\mathcal{Q}_{\pi^0} = 1/3$  for  $\pi^0$ ,  $\mathcal{Q}_{\eta_u} = 5/9$  for  $\eta_u$ , and  $\mathcal{Q}_{\eta_s} = -\sqrt{2}/9$  for  $\eta_s$ ;  $S$  is the quark propagator:

$$S^{-1}(k; m_a) = \not{k} - m_a \quad (23)$$

with the constituent quark mass  $m_a = m_u$  for  $P = \pi$  or  $P = \eta_u$  and  $m_a = m_s$  for  $P = \eta_s$ . Comparing (22) with (1), one obtains:

$$\mathcal{F}_P(q_1^2, q_2^2, p^2) = \frac{g_P}{2\pi^2} m_a I_{P\gamma\gamma}(q_1^2, q_2^2, p^2). \quad (24)$$

---

<sup>2)</sup>The strange quark mass can be fixed also from the  $\phi$ -meson mass [24]

The Feynman integral  $I_{P\gamma\gamma}(q_1^2, q_2^2, p^2)$  is given (in Euclidean metric) by

$$I_{P\gamma\gamma}(q_1^2, q_2^2, p^2) = \int \frac{d^4k}{\pi^2} \frac{\theta(\Lambda_{\text{NJL}}^2 - k^2)}{[m_a^2 + (k + p/2)^2][m_a^2 + (k - p/2)^2][m_a^2 + (k - (q_1 - q_2)/2)^2]}. \quad (25)$$

In the chiral limit  $p^2 = 0$ , when both photons are on-mass-shell ( $q_1^2 = q_2^2 = 0$ ), integral (25) becomes very simple. Formally, it is finite, and one can set the UV cut-off  $\Lambda_{\text{NJL}}$  to infinity, and thus obtain that it is equal to  $1/(2m_a^2)$ . As a result, one reproduces the well-known result for the decay  $\pi^0 \rightarrow \gamma\gamma$  (see (2)). For the  $\eta$  and  $\eta'$  mesons, the result is similar, and the only difference is that the singlet-octet mixing should be taken into account:

$$\mathcal{F}_\eta(0, 0, 0) = \frac{1}{4\pi^2 \tilde{f}_\eta}, \quad \mathcal{F}_{\eta'}(0, 0, 0) = \frac{1}{4\pi^2 \tilde{f}_{\eta'}}, \quad (26)$$

$$\tilde{f}_\eta^{-1} = \frac{5}{3f_u} \sin(\theta_0 - \theta) - \frac{\sqrt{2}}{3f_s} \cos(\theta_0 - \theta) \quad (27)$$

$$\tilde{f}_{\eta'}^{-1} = \frac{5}{3f_u} \cos(\theta_0 - \theta) + \frac{\sqrt{2}}{3f_s} \sin(\theta_0 - \theta). \quad (28)$$

Here, the meson weak decay constants are  $f_u \equiv f_\pi$ , and  $f_s = m_s/g_s \approx 1.25f_u$ . Thus, we have  $\tilde{f}_\eta = 83$  MeV and  $\tilde{f}_{\eta'} = 73$  MeV. (For the discussion of singlet-octet mixing see [25])

Let us now consider the high virtuality region:  $Q^2 \rightarrow \infty$  (see (3) for definition). We estimate the asymptotics of the transition form factor. Let us rewrite the expression for integral (25) by using the Feynman  $\alpha$ -parameterization for the denominators and integrating over the angular variables. Then, the corresponding integral  $I_{P\gamma\gamma}$  is given by

$$I_{P\gamma\gamma}(q_1^2, q_2^2, p^2) = \int_0^{\Lambda_{\text{NJL}}^2/m_q^2} \frac{u du}{m_q^2 + u - \frac{p^2}{4}} \times \int_0^1 d\alpha \left[ \frac{1}{\sqrt{b^4 - a_+^4} (b^2 + \sqrt{b^4 - a_+^4})} + \frac{1}{\sqrt{b^4 - a_-^4} (b^2 + \sqrt{b^4 - a_-^4})} \right], \quad (29)$$

where  $u = k^2$  and

$$b^2 = m_a^2 + u + \frac{1}{2}\alpha Q^2 - \frac{1}{4}(1 - 2\alpha)p^2, \quad a_\pm^4 = 2u\alpha Q^2 (\alpha \pm \omega(1 - \alpha)) - (1 - 2\alpha)u p^2. \quad (30)$$

In this way, the expression (29) can be safely analyzed in the asymptotic limit of high total virtuality of the photons  $Q^2 \rightarrow \infty$ . Moreover, the integral over  $\alpha$  can be taken analytically, leading, in the chiral limit  $p^2 = 0$ , to the asymptotic expression given by (5), where (see [16])

$$J_P(\omega) \equiv J_{P,\text{np}}(\omega) = \frac{g_P^2 \mathcal{Q}_{PZ}}{8\pi^2 \omega} \left\{ \int_0^{\Lambda_{\text{NJL}}^2/m_q^2} \frac{du}{1+u} \ln \left[ \frac{1+u(1+\omega)}{1+u(1-\omega)} \right] \right\} \quad (31)$$

$$a = u \text{ if } P = \pi, \eta_u, \text{ and } a = s \text{ if } P = \eta_s. \quad (32)$$

The  $\eta$  and  $\eta'$  mesons appear as mixed  $\eta_u$  and  $\eta_s$  states (see (14)), and for them, one has:

$$J_\eta(\omega) = c_1 J_{\eta_u}(\omega) + c_2 J_{\eta_s}(\omega), \quad (33)$$

$$J_{\eta'}(\omega) = c_3 J_{\eta_u}(\omega) + c_4 J_{\eta_s}(\omega), \quad (34)$$

where the coefficients  $c_i$  are:

$$\begin{aligned} c_1 &= \frac{5f_u}{3f_\eta} \sin(\theta_0 - \theta), & c_2 &= -\frac{\sqrt{2}f_s}{3f_\eta} \cos(\theta_0 - \theta), \\ c_3 &= \frac{5f_u}{3f_{\eta'}} \cos(\theta_0 - \theta), & c_4 &= \frac{\sqrt{2}f_s}{3f_{\eta'}} \sin(\theta_0 - \theta), \end{aligned} \quad (35)$$

and the constants  $f_\eta$  and  $f_{\eta'}$  are defined as <sup>3)</sup>

$$f_\eta = \frac{5}{3}f_u \sin(\theta_0 - \theta) - \frac{\sqrt{2}}{3}f_s \cos(\theta_0 - \theta) = 95 \text{ MeV}, \quad (36)$$

$$f_{\eta'} = \frac{5}{3}f_u \cos(\theta_0 - \theta) + \frac{\sqrt{2}}{3}f_s \sin(\theta_0 - \theta) = 135 \text{ MeV}. \quad (37)$$

One should also note an extra factor  $Z$  in the expression of  $J_P(\omega)$  in (31). Analogously, the factor  $Z$  appears in the amplitude of the decay  $\pi \rightarrow \mu\tilde{\nu}_\mu$  that determines the pion weak coupling constant  $f_\pi$ . To obtain a correct result, one should take account of  $\pi - a_1$  transitions by considering additional contributions going from the diagrams with axial-vector type vertices (see the term  $L_2$  in (11)). When calculating both the  $\pi \rightarrow \mu\tilde{\nu}_\mu$  amplitude and the  $\gamma^* \rightarrow P\gamma^*$  transition form factor, the account of  $\pi - a_1$  transitions leads to cancelation of the factor  $Z$ .

### 3.3. Distribution amplitudes of pseudoscalar mesons.

The quark-meson interaction in the NJL model [2] is described by the vertices given in (7)–(12). One just has to calculate the integral (25). Formally, the integral (25) is convergent, and an UV cut-off is not necessary here, however, the extracting of its asymptotic behavior at large  $Q^2$  would lead to logarithmic dependence  $\sim (\ln Q^2)^2/Q^2$ , which is not expected, as it is known from QCD. Therefore, the UV cut-off in the NJL model should be treated not only as a trick to make the integrals convergent, but also as a way to take into account the nontrivial nonlocal vacuum structure. The UV cut-off also forbids the large momenta flow through meson vertices.

From (31) it is clear that the prediction of the nonperturbative approach to the asymptotic coefficient  $J_P(\omega)$  is rather sensitive to the ratio of the ultra-violet cut-off  $\Lambda_{\text{NJL}}$  to the value of the constituent mass  $m_a$  and to the relative distribution of the total virtuality among photons,  $\omega$ . In particular, for the off-shell process  $\gamma^* \rightarrow \pi^0\gamma^*$  in the kinematic case of symmetric distribution of photon virtualities,  $q_1^2 = q_2^2 \rightarrow -\infty$  ( $\omega \rightarrow 0$ ), the result  $J(|\omega| = 0) = 4/3$  obtained from (31) is in agreement with the OPE prediction.

---

<sup>3)</sup> Note that the definition of  $f_\eta$  and  $f_{\eta'}$  differs from that of  $\tilde{f}_\eta$  and  $\tilde{f}_{\eta'}$  (see (27) and (28)).



Integral (25) is similar in its structure to the integral arising in the lowest order of pQCD treating the quark-photon interaction perturbatively. In the latter case, its asymptotic behavior is due to the subprocess  $\gamma^*(q_1) + \gamma^*(q_2) \rightarrow \bar{q}(\bar{x}p) + q(xp)$  with  $x$  ( $\bar{x} = 1 - x$ ) being the fraction of the meson momentum  $p$  carried by the quark produced at the  $q_1$  ( $q_2$ ) photon vertex. The relevant diagram is similar to the handbag diagram for hard exclusive processes, with the main difference that one should use, as a nonperturbative input, a quark-meson vertex instead of the meson DA. As we see below, this similarity allows one to reconstruct the shape of the meson DA.

Both the expressions for  $J_P$  derived within the quark-meson model (31) and from the light-cone OPE (6) can be put into the common form

$$J_P(\omega) = \frac{2}{3\omega} \int_0^1 d\xi R_P(\xi) \ln \left[ \frac{1 + \xi\omega}{1 - \xi\omega} \right] \quad (38)$$

with

$$R_P^{\text{pQCD}}(\xi) = -\frac{d}{d\xi} \varphi_P^A \left( \frac{1 + \xi}{2} \right) \quad \text{and} \quad R_{P,\text{np}}(\xi) = 16\pi^2 g_a^2 \theta \left( 1 - \frac{\xi}{1 - \xi} \frac{m_a^2}{\Lambda_{\text{NJL}}^2} \right) \frac{1}{1 - \xi}, \quad (39)$$

where  $0 \leq \xi \equiv (2x - 1) \leq 1$

and similar expressions for  $-1 \leq \xi \leq 0$ . Equating both the contributions, we find the meson DA

$$\varphi_P^A(x) = \frac{g_a^2}{4\pi^2} \int_{|2x-1|}^1 \theta \left( 1 - \frac{y}{1-y} \frac{m_a^2}{\Lambda_{\text{NJL}}^2} \right) \frac{dy}{1-y}. \quad (40)$$

Thus, we show that (31) obtained within the NJL model is equivalent to the standard lowest-order pQCD result (6), with the only difference that the nonperturbative information accumulated in the meson DA  $\varphi_P^A(x)$  in pQCD is represented in NJL by the quark-meson vertex and is connected with the regularization procedure.

Within the NJL model, from (40) one can easily obtain analytic expressions for two special DA describing the distribution of  $u(d)$ - and  $s$ -quarks, respectively,

$$\varphi_u^A(x) = \begin{cases} \frac{\ln \left| \frac{1 - \xi_u}{1 - |2x - 1|} \right|}{\xi_u + \ln |1 - \xi_u|}, & |2x - 1| \leq \xi_u \\ 0, & |2x - 1| > \xi_u \end{cases} \quad (41)$$

where the constant  $\xi_u$  is defined as follows:

$$\xi_u = \frac{\Lambda_{\text{NJL}}^2}{\Lambda_{\text{NJL}}^2 + m_u^2}; \quad (42)$$

$$\varphi_s^A(x) = \begin{cases} \frac{\ln \left| \frac{1 - \xi_s}{1 - |2x - 1|} \right|}{\xi_s + \ln |1 - \xi_s|}, & |2x - 1| \leq \xi_s, \\ 0, & |2x - 1| > \xi_s \end{cases}, \quad (43)$$

$$\xi_s = \frac{\Lambda_{\text{NJL}}^2}{\Lambda_{\text{NJL}}^2 + m_u^2}. \quad (44)$$

For the pion,  $\eta$ , and  $\eta'$  mesons, one has:

$$\varphi_\pi(x) = \varphi_u^A(x), \quad (45)$$

$$\varphi_\eta(x) = c_1 \varphi_u^A(x) + c_2 \varphi_s^A(x), \quad (46)$$

$$\varphi_{\eta'}(x) = c_3 \varphi_u^A(x) + c_4 \varphi_s^A(x), \quad (47)$$

where the coefficients  $c_i$  are defined in (35). The DA calculated in the NJL are shown in Figs. 2–5.

### 3.4. Instanton-induced effective quark-meson Lagrangian

Let us consider now the piece of the effective quark-meson Lagrangian that appears in IQM. The effective quark-meson dynamics can be summarized in the covariant nonlocal action given by

$$S_{\text{int}} = - \int d^4x d^4y F [x + y/2, x - y/2; \Lambda_{\text{IQM}}^{-2}] \times \\ \times \bar{q}(x + y/2) i\gamma_5 [g_{\pi\bar{q}q} \sum_{a=1}^3 \lambda^a \pi^a(x) + g_{\eta_u} \lambda_u \eta_u(x) + g_{\eta_s} \lambda_s \eta_s(x)] q(x - y/2). \quad (48)$$

The dynamic vertex  $F [x + y/2, x - y/2; \Lambda_{\text{IQM}}^{-2}]$  depends on the coordinates of the quark and antiquark and arises due to the quark-antiquark interaction induced by exchange of instanton with size  $\Lambda_{\text{IQM}}^{-1} \simeq \rho_c$ ,  $\Lambda_{\text{IQM}} \approx 0.742$  GeV. The nonlocal vertex characterizes the coordinate dependence of order parameter for SBCS and can be expressed in terms of the nonlocal quark condensates.

We restrict ourselves to the approximation (see, e.g. [26])

$$F [x + y/2, x - y/2; \Lambda_{\text{IQM}}^{-2}] \rightarrow F(y^2, \Lambda_{\text{IQM}}^{-2}), \quad (49)$$

when the dynamic quark-meson vertex depends only on the relative coordinate of the quark and antiquark squared,  $y^2$ , if neglecting the dependence of the vertex on the angular variable ( $yx$ ). The Fourier transform of the vertex function in the Minkowski space is defined as  $\tilde{F}(k^2; \Lambda_{\text{IQM}}^2) = \int d^4x F(x^2; \Lambda_{\text{IQM}}^{-2}) \exp(-ikx)$  with normalization  $\tilde{F}(0; \Lambda_{\text{IQM}}^2) = 1$ , and we assume that it rapidly decreases in the Euclidean region ( $k^2 = -k_E^2 \equiv -u$ ). As in the NJL model, we also approximate the momentum-dependent quark self-energy in the quark propagator  $S^{-1}(k; m_a) = \not{k} - m_a$  by a constant quark mass [26] and neglect meson mass effects. The

quark masses are  $m_u = 275$  MeV,  $m_s = 430$  MeV, close to those obtained in the NJL model (see Sect. 3.1.). We have to note that the approximations used here are not fully consistent. Further, as the reader will see below, the choice of the model for the quark-meson vertex (49), depending only on the relative coordinate, induces a certain artifact in the  $x$  behaviour of DA. However, these deficiencies of the chosen approximation are not essential for the present purpose and do not lead to large numerical errors.

The quark-meson coupling is given by the condition [26]

$$g_q^{-2} = \frac{N_c}{8\pi^2} \int_0^\infty du u \tilde{F}^2(-u; \Lambda_{\text{IQM}}^2/m_q^2) \frac{3+2u}{(1+u)^3}; \quad (50)$$

and the meson weak decay constants  $f_\pi \equiv f_u$ , and  $f_s$  are expressed by

$$f_q = \frac{N_c g_q}{4\pi^2} M_q \int_0^\infty du u \tilde{F}(-u; \Lambda_{\text{IQM}}^2/m_q^2) \frac{1}{(1+u)^2}. \quad (51)$$

We have rescaled the integration variable by the quark mass squared. Within the instanton vacuum model, the size of nonlocality of the nonperturbative gluon field,  $\rho_c \sim \Lambda_{\text{IQM}}^{-1} \simeq 0.3$  fm, is much smaller than the quark Compton length  $m_q^{-1}$ .

To calculate the transition form factors, one can use the same formulas that have been obtained above in the NJL model. The only exception is that the  $\theta$ -function should be replaced by the nonlocal quark-meson vertex function  $\tilde{F}(-u, \Lambda_{\text{IQM}}^2/m_q^2)$ . In the next section, we discuss numerical results obtained in IQM as compared with the NJL model calculation and experimental data.

Let us note that we use an approximation to the model with constant constituent quark masses for all three quark lines in the diagrams of the process (see Fig. 1). However, the asymptotic result (31) is independent of the mass in the quark propagator with hard momentum flow, as it should be. The other two quark lines remain soft during the process; thus, the mass  $m_a$  can be considered as given on a certain characteristic soft scale in the momentum-dependent case  $m_a$ .

#### 4. DISCUSSION AND CONCLUSION

Within the two ECQM under consideration that describe the quark-meson dynamics, we calculated the  $\gamma^* \rightarrow P\gamma^*$  transition form factor at moderately high momentum transfers squared in a wide kinematic domain. From the model calculations, the normalization coefficient  $J_P(\omega)$  of the leading  $Q^{-2}$  term is found (see (31)). It depends on the ratio of the constituent quark mass to the UV cut-off  $\Lambda$  and also on the kinematics of the process. From the comparison of the kinematic dependence of the asymptotic coefficient of the transition form factors, given by pQCD and NJL, the meson distribution amplitudes (40) are derived. Analogously, a relation between DA and the dynamic quark-meson vertex function is obtained in IQM. In the specific case of symmetric kinematics ( $q_1^2 = q_2^2$ ), our result agrees with the one

obtained by OPE and also with the expression for the constant  $f_P$  that determines the decay  $P \rightarrow \mu\tilde{\nu}_\mu$  of meson  $P$ .

Let us discuss DA obtained in different approaches. In the NJL, we obtained explicit expressions for the DA of pion,  $\eta$ , and  $\eta'$  meson. They are plotted in Figs. 2–4 (solid line) from where one can see that the NJL model predicts a more flat distribution of quark momenta in a meson than IQM. To compare with other theoretical approaches, we also plotted, as a sample, the results obtained in IQM (dashed line). There are also given the asymptotic pQCD expression for DA:  $\phi^{\text{asympt}}(x) = 6x(1-x)$  (dashed-dotted line). One can see that for the most of  $x$ , the DA's shapes are similar in different approaches. The difference can be noticed near  $x \approx 1/2$  and at the edges. The cusp at  $x = 1/2$  and a very sharp decrease of DA near  $x = 0$  and  $x = 1$  are artifacts closely related to the UV regularization in the NJL model and to the shape of the nonlocal quark-meson vertex function in IQM. However, these deficiencies turned out to be not crucial in our calculations.

Now, we would like to make some notes regarding the definition of  $f_\eta$  and  $f_{\eta'}$  used by authors of [15]. In [15],  $f_P$  are obtained from the tabulated data on the decays  $P \rightarrow \gamma\gamma$ , using the low-energy limit of the process amplitude

$$\mathcal{F}_P(0, 0, 0) \simeq 1/(4\pi^2\tilde{f}_P) \quad (52)$$

(see (6) in [15]). This works well for the pion, but the case of the  $\eta$  and  $\eta'$  mesons is rather different because of the singlet-octet mixing. In the limit  $Q^2 \rightarrow \infty$ , one should expect:

$$\lim_{Q^2 \rightarrow \infty} Q^2 \mathcal{F}_P(q_1^2 = -Q^2, q^2 = 0, p^2 = 0) = 2f_P, \quad (53)$$

where  $f_P$  are not the same as  $\tilde{f}_P$  except for  $f_\pi$  as one can see from comparing (36) and (37) with (27) and (28). That is why the CLEO fit noticeably disagrees with the limit  $2f_{\eta'}$  (see (5) in [15]) drawn in Fig. 23 [15]. Therefore, it is not correct to use the equation (7) in [15] to perform a fit. From our calculation, we see that, taking into account the singlet-octet mixing, one can avoid the discrepancy in the description of the  $\gamma^* \rightarrow P\gamma$  interaction both at small and large  $Q^2$ .

Now we compare our results for the case  $\omega = 1$  ( $\gamma^* \rightarrow P\gamma$ ) with those given by the CLEO collaboration [15] for large  $Q^2$ . We calculate the product of  $Q^2$  and transition form factor:

$$\mathcal{F}_P(\omega) = \lim_{Q^2 \rightarrow \infty} Q^2 \mathcal{F}_P(q_1^2, q_2^2, p^2). \quad (54)$$

Theoretically we have

$$\mathcal{F}_P(\omega) = J_P(\omega)f_P, \quad (55)$$

according to (5). In the NJL model,  $J_\pi(1) = 1.97$ ,  $J_\eta(1) = 2.04$ ,  $J_{\eta'}(1) = 1.9$ . Therefore,  $\mathcal{F}_\pi(1) \approx 0.184$  GeV,  $\mathcal{F}_\eta(1) \approx 0.193$  GeV, and  $\mathcal{F}_{\eta'}(1) \approx 0.256$  GeV. The IQM predicts  $J_\pi(1) = 1.78$ ,  $J_\eta(1) = 1.83$ ,  $J_{\eta'}(1) = 1.73$  and  $\mathcal{F}_\pi(1) \approx 0.16$  GeV,  $\mathcal{F}_\eta(1) \approx 0.17$  GeV, and  $\mathcal{F}_{\eta'}(1) \approx 0.23$  GeV.

The infinite value of  $Q^2$  cannot be reached in experiment, so we determine  $\mathcal{F}_P(\omega)$  at the value of  $Q^2$ , maximum accessible in experiment. Thus, the CLEO collaboration gives

$\mathcal{F}_\pi(1) = 0.17 \pm 0.3$  GeV at  $Q^2 = 7.0 - 9.0$  GeV<sup>2</sup>,  $\mathcal{F}_\eta(1) \approx 0.16$  GeV at  $Q^2 \sim 22$  GeV<sup>2</sup>,  $\mathcal{F}_{\eta'}(1) \approx 0.25$  GeV at  $Q^2 \sim 30$  GeV<sup>2</sup>. The monopole interpolation for the transition form factors (5) obtained both theoretically and experimentally is shown in Figs. 6–8. One can see, that the experiment gives values for the transition form factors lower than models. The biggest difference (about 20 %) displays for the  $\eta$  meson. The best agreement of models with the CLEO fit is obtained for  $\pi$  and  $\eta'$ .

The constants  $g_{P\gamma\gamma}$  in the monopole Ansatz (5) for the transition form factors are related with the  $P \rightarrow \gamma\gamma$  decay width. It is interesting to compare their values predicted in different models with experimental data. According to (52), we obtain from NJL:  $g_{\pi\gamma\gamma} = 0.27$  GeV<sup>-1</sup>,  $g_{\eta\gamma\gamma} = 0.31$  GeV<sup>-1</sup>, and  $g_{\eta'\gamma\gamma} = 0.35$  GeV<sup>-1</sup>. The same gives us IQM. From experiment we have  $g_{\pi\gamma\gamma}^{\text{exp}} = 0.26$  GeV<sup>-1</sup>,  $g_{\eta\gamma\gamma}^{\text{exp}} = 0.26$  GeV<sup>-1</sup>, and  $g_{\eta'\gamma\gamma}^{\text{exp}} = 0.34$  GeV<sup>-1</sup>. Again, the model prediction for  $\pi$  and  $\eta'$  better suits to the experimental values, whereas for the  $\eta$  meson, one has a noticeable discrepancy.

The results presented in our paper are in accordance with the conclusions made in [12, 14, 27] within the QCD sum rules, which evidences that our approach is valid for the process under consideration and makes us hope that it can be applied to other processes with large momentum transfers, as well.

We plan to use the ECQM approach approved here on the process  $\gamma^* \rightarrow P\gamma$ , for the description of the following processes:  $\gamma^* \rightarrow P\rho$ ,  $\gamma^* \rightarrow P\omega$ ,  $\gamma^* \rightarrow P'\gamma$  (with  $P'$  being a radial excitation of a pseudoscalar meson),  $\gamma^* \rightarrow S\gamma$  (with  $S$  being a scalar meson),  $\gamma^* \rightarrow \gamma A$  (with  $A$  being an axial-vector meson),  $\gamma^* \rightarrow \gamma\pi\sigma$ ,  $\gamma^* \rightarrow \gamma\pi\rho$ ,  $\gamma^*\gamma^* \rightarrow \pi\pi$  etc.

The work is supported by the Heisenber-Landau program and RFBR Grants 01-02-16231 and 02-02-16194 and by Grant INTAS-2000-366.

## REFERENCES

1. M.K.Volkov, Ann. Phys. **49**, 202 (1986).
2. M.K. Volkov, Sov. J. Part. Nucl. **17**, 186 (1986).
3. D. Ebert, H. Reinhardt, and M.K. Volkov, Prog. Part. Nucl. Phys. **35**, 1 (1994).
4. H. Vogl and W. Weise, Progr. Part. Nucl. Phys. **27**, 195 (1991).
5. S.P. Klevansky Rev. Mod. Phys. **64**, 649 (1992).
6. M.K. Volkov and V.L. Yudichev, Fiz. Elem. Chast. Atom. Yadra **31**, 576 (2000).
7. M.K.Volkov and V.L.Yudichev, Eur. Phys. J. A **10**, 109 (2001).
8. M.K.Volkov and V.L.Yudichev, Eur. Phys. J. A **10**, 223 (2001).
9. V.L. Chernyak and A.R. Zhitnitsky, JETP Lett. **25**, 510 (1977)
10. A.V. Efremov and A.V. Radyushkin, Math. Phys. **42**, 97 (1980); *ibid* Phys. Lett. B **94**, 45 (1980).
11. S.J. Brodsky and G.P. Lepage, Phys. Lett. B **87**, 359 (1979); *ibid* Phys. Rev. D **22**, 2157 (1980).
12. S.V. Mikhailov and A. V. Radyushkin, Sov. J. Nucl. Phys. **52**, 697 (1990).
13. S.V. Mikhailov and A.V. Radyushkin, JETP Lett. **43**, 712 (1986); Sov.J.Nucl. Phys. **49**, 494 (1989); Phys. Rev. D **45**, 1754 (1992).
14. A. V. Radyushkin and R. T. Ruskov, Nucl. Phys. B **481**, 625 (1996); hep-ph/9706518.
15. J. Gronberg *et. al.*, (*CLEO Collab.*), Phys. Rev. D **57**, 33 (1998).
16. I.V. Anikin, A.E. Dorokhov, and Lauro Tomio, Phys. Let. B **475**, 361 (2000); A.E. Dorokhov and Lauro Tomio, Phys. Rev. D **62**, 014016 (2000); I.V. Anikin, A.E. Dorokhov, and L. Tomio, Phys. Part. Nucl. **31**, 509 (2000); I.V.Anikin, O.V.Teryaev, Phys. Lett. B **509**, 95 (2001).
17. S. Adler, Phys. Rev. **177**, 2426 (1969).
18. J.S. Bell and R. Jackiw, Nuovo Cim. A **60**, 47 (1969).
19. G. P. Lepage and S. J. Brodsky, Phys. Lett. B **87**, 359 (1979); Phys. Rev. D **22**, 2157 (1980).
20. M.K. Volkov and V.L. Yudichev, Nuovo Cim. A **112**, 225 (1999).

21. D.E. Groom *et. al* Eur. Phys. J C **15**, 1 (2000).
22. T. Eguchi, Phys. Rev. D **14**, 2755 (1976).
23. K. Kikkawa, Prog. Theor. Phys. **56**, 947 (1976).
24. M.K. Volkov and A.N. Ivanov, Theor. Math. Phys. **69**, 1066 (1986).
25. Th. Feldmann and P. Kroll, hep-ph/0201044.
26. H. Ito, W.W. Buck, F. Gross, Phys. Rev. C **45**, 1918 (1992); Phys. Lett. B **287**, 23 (1992); I. Anikin, M. Ivanov, N. Kulimanova, V. Lyubovitskii, Phys. Atom. Nucl. **57**, 1082 (1994).
27. A.P. Bakulev, S.V. Mikhailov, Phys. Lett. B **436**, 351 (1998).

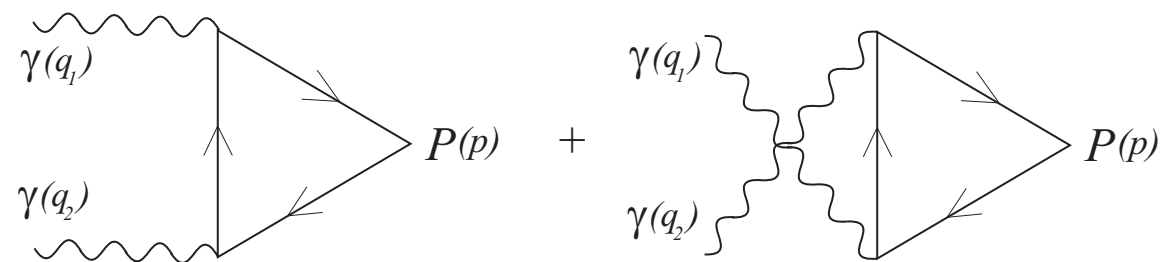
## FIGURE CAPTIONS

1. The diagrams contributing to the process  $\gamma^*\gamma^* \rightarrow P$  ( $\gamma^* \rightarrow P\gamma^*$ ) amplitude.
2. The DA  $\varphi_u$  in the NJL and IQM models and the asymptotic DA.
3. The DA  $\varphi_s$  in the NJL and IQM models and the asymptotic DA.
4. The DA  $\varphi_\eta$  in the NJL and IQM models and the asymptotic DA.
5. The DA  $\varphi_{\eta'}$  in the NJL and IQM models and the asymptotic DA.
6. The light-cone transition form factor for the pion. The solid line corresponds to the NJL-model calculation, the dashed line is a fit to the CLEO data, the dashed-dotted line is corresponds to IQM, and the dotted line is  $2f_\pi$ .
7. The light-cone transition form factor for the  $\eta$  meson. The solid line corresponds to the NJL-model calculation, the dashed line is a fit to the CLEO data, the dashed-dotted line is corresponds to IQM, and the dotted line is  $2f_\eta$ .
8. The light-cone transition form factor for the  $\eta'$  meson. The solid line corresponds to the NJL-model calculation, the dashed line is a fit to the CLEO data, the dashed-dotted line is corresponds to IQM, and the dotted line is  $2f_{\eta'}$ .



FIGURES

Figure 1:



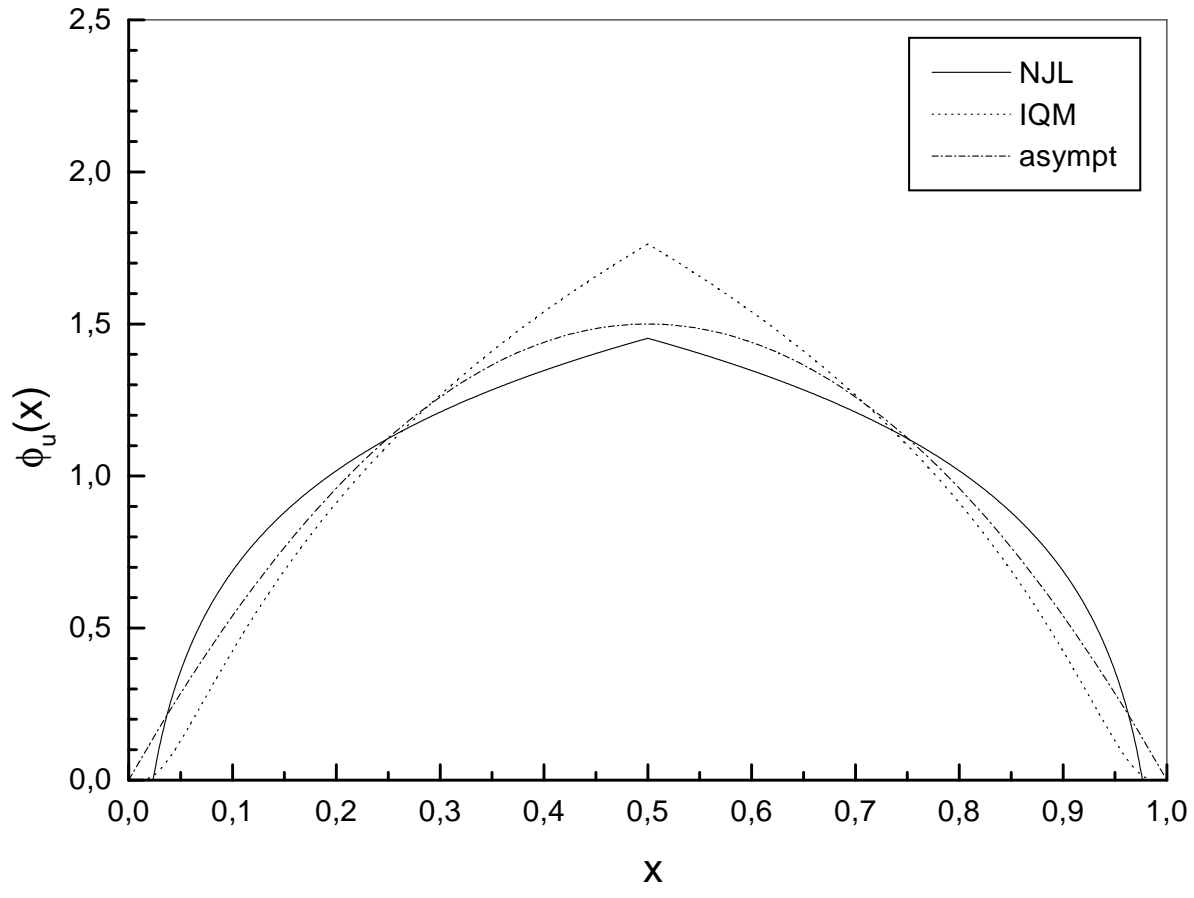


Figure 2:

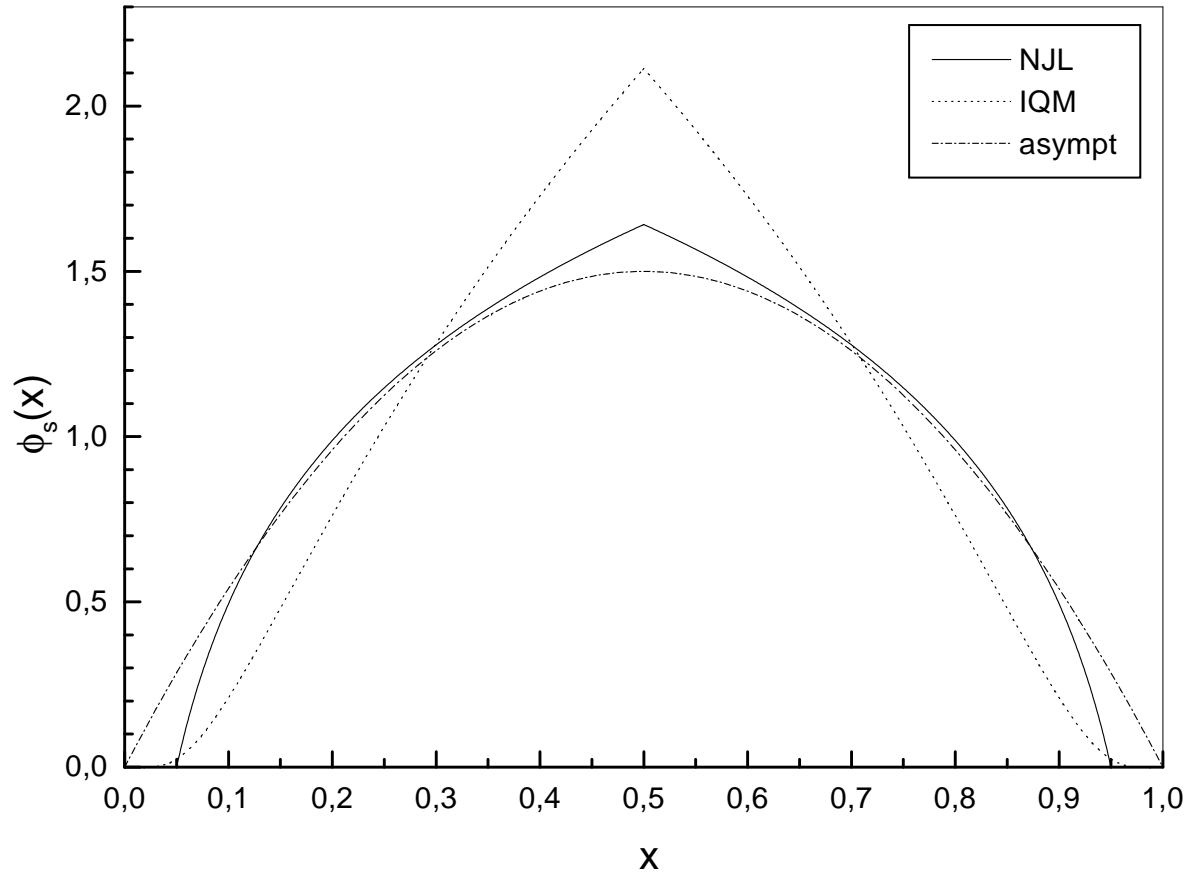


Figure 3:

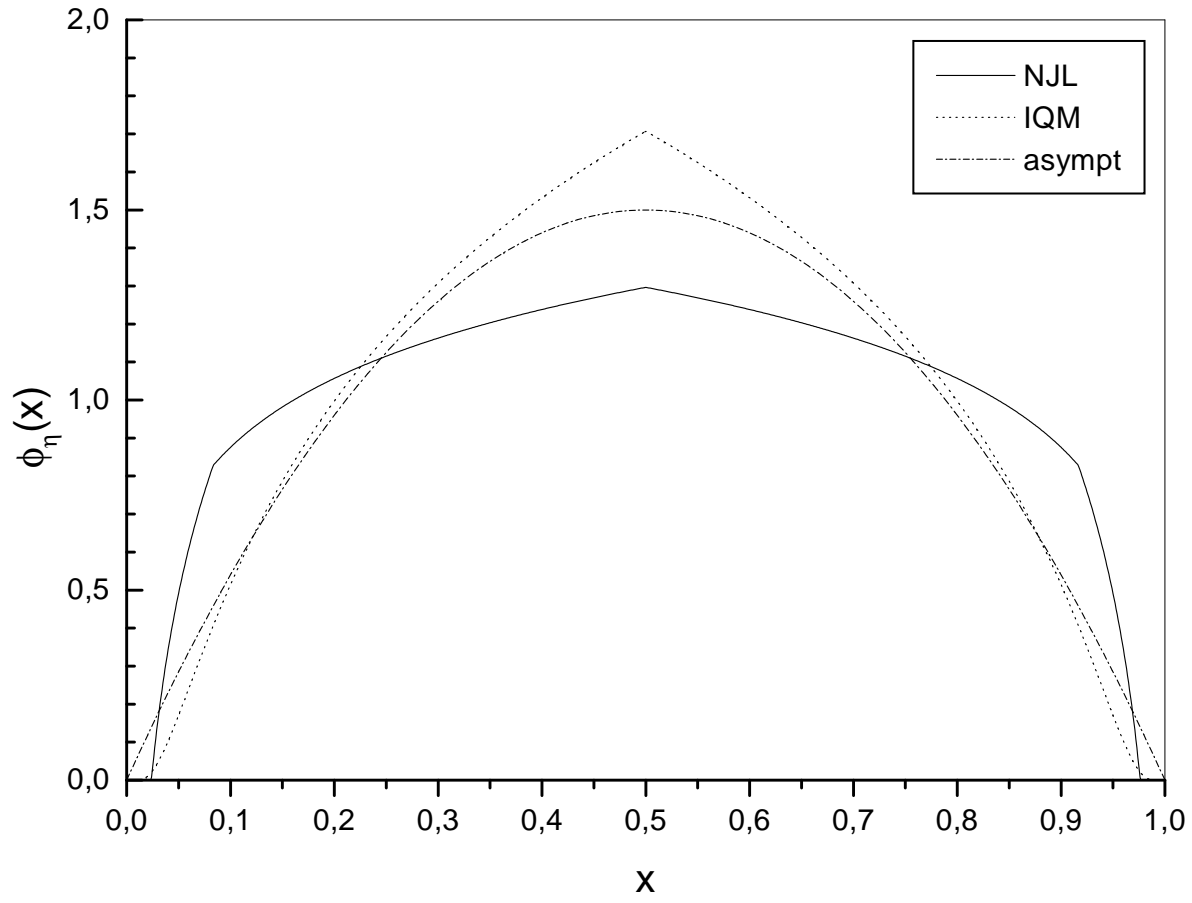


Figure 4:

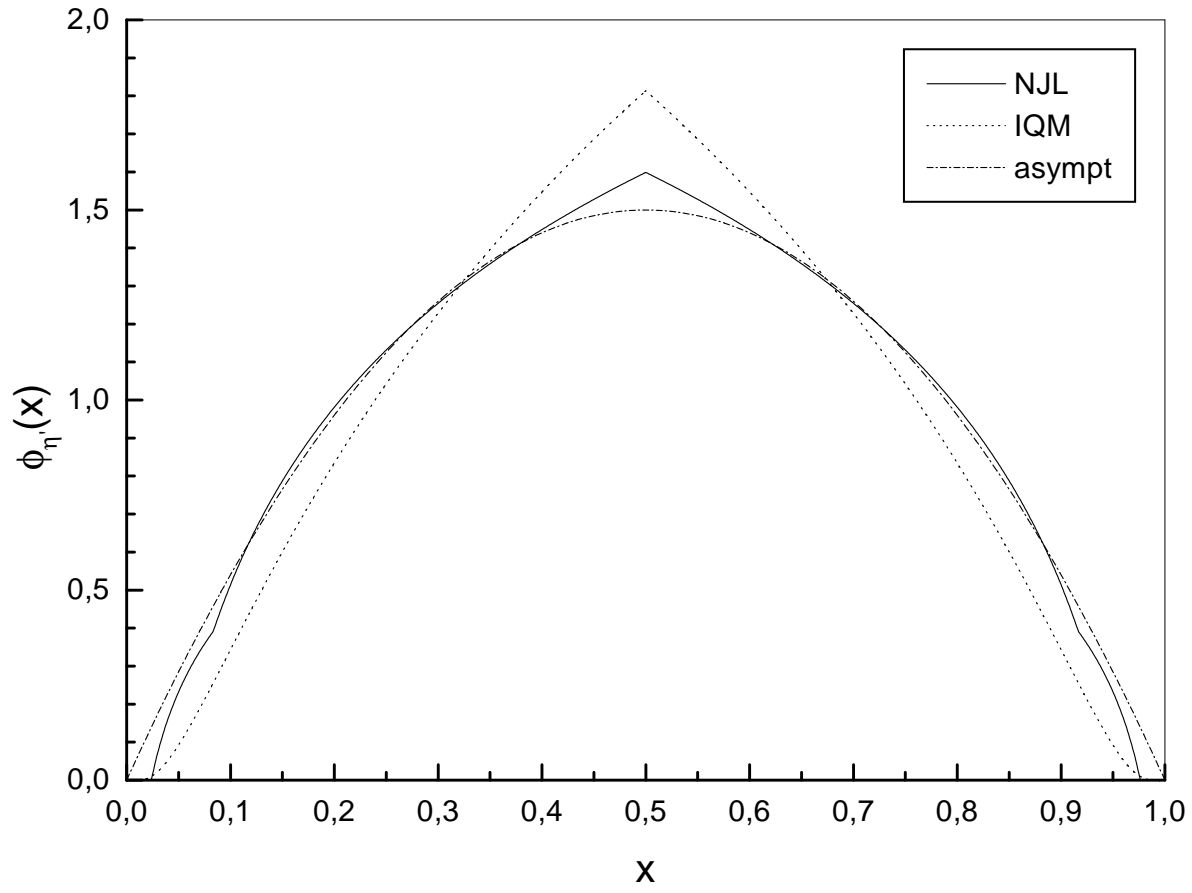


Figure 5:

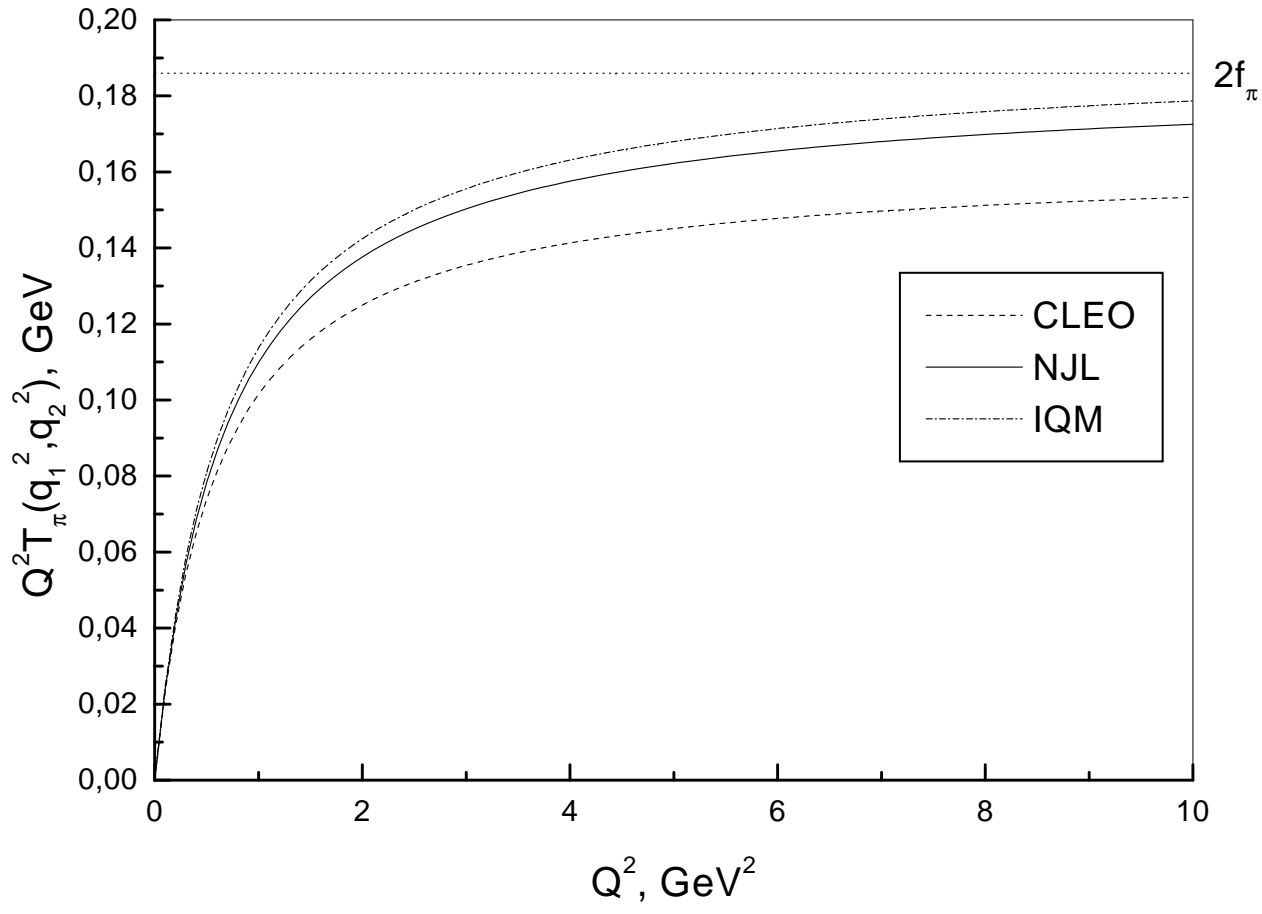


Figure 6:

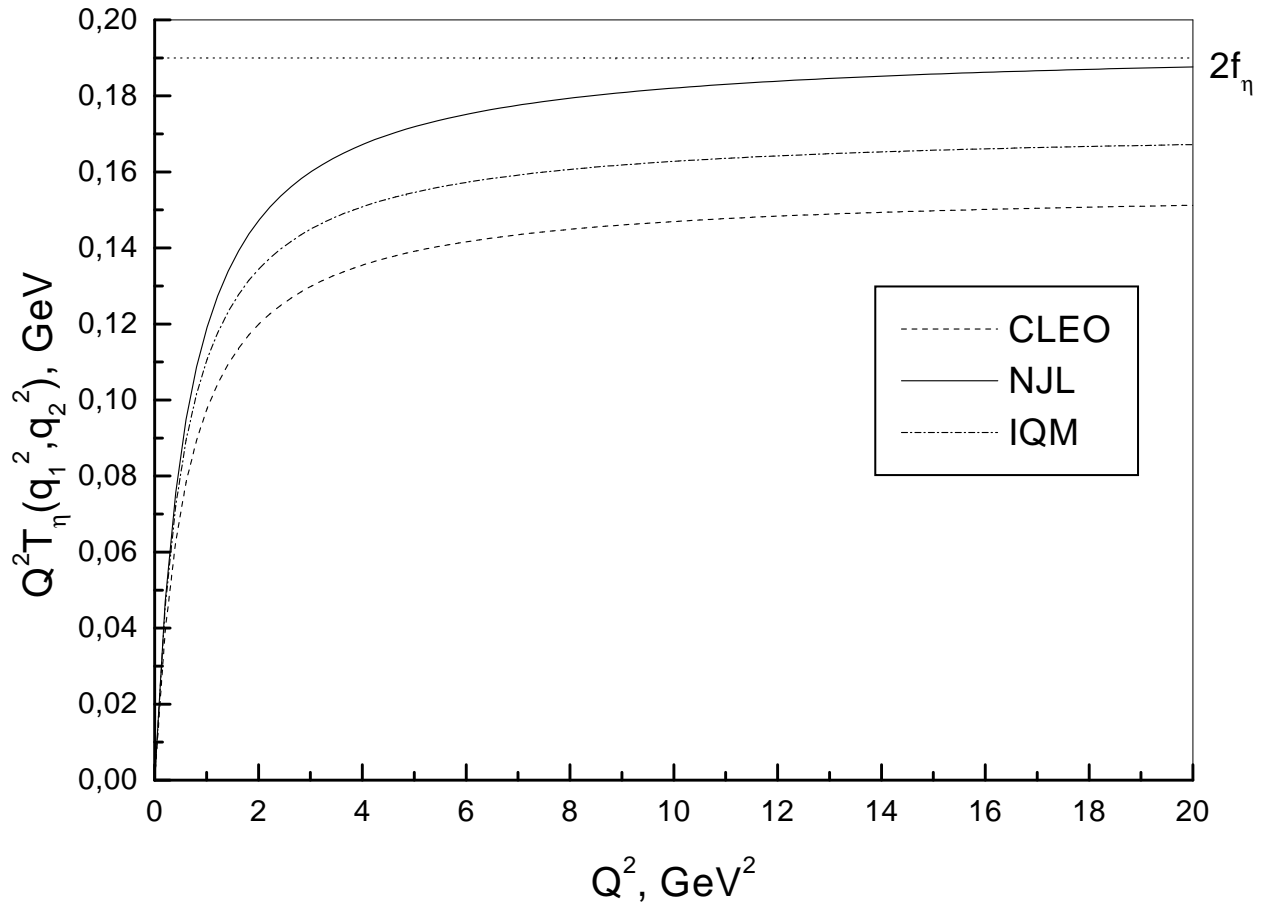


Figure 7:

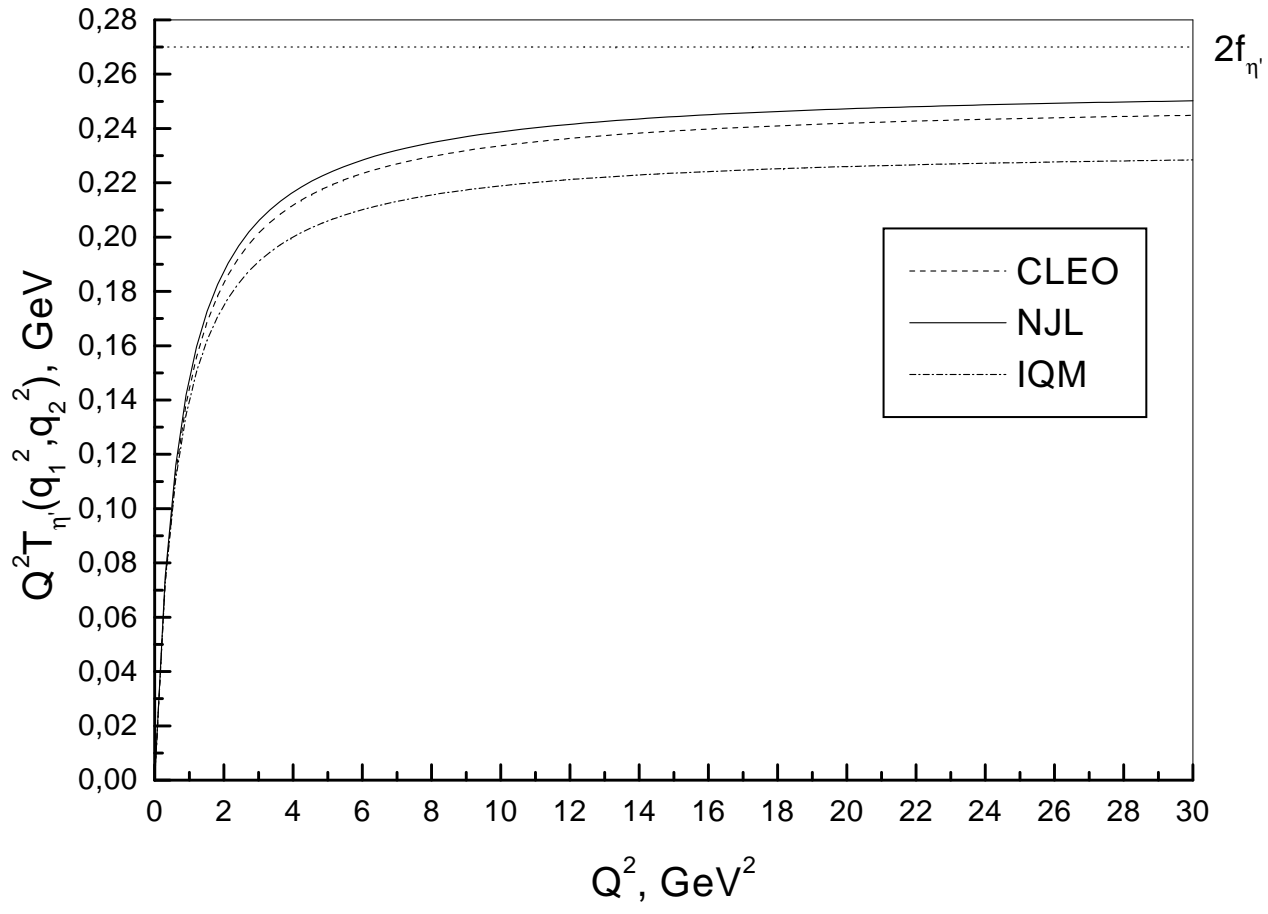


Figure 8: